Polymer 51 (2010) 3851–3858

Contents lists available at ScienceDirect

Polymer

journal homepage: www.elsevier.com/locate/polymer

Synthesis and characterization of organo-soluble thioether-bridged polyphenylquinoxalines with ultra-high refractive indices and low birefringences

Cheng Li, Zhuo Li, Jin-gang Liu*, Xiao-juan Zhao, Hai-xia Yang, Shi-yong Yang*

Laboratory of Advanced Polymer Materials, Institute of Chemistry, Chinese Academy of Sciences, Beijing 100190, China

ARTICLE INFO

Article history:
Received 9 February 2010
Received in revised form
18 June 2010
Accepted 18 June 2010
Available online 1 July 2010

Keywords:
Polyphenylquinoxaline
Thioether
High refractive index

ABSTRACT

Two aromatic tetraketones, 4,4′-thiobis[(*p*-phenyleneoxy)benzil] (STK, 1) and 4,4′-thiobis[(*p*-phenylenesulfanyl)benzil] (3STK, 2) were synthesized by the nitro nucleophilic substituent reactions of 4-nitrobenzil and corresponding diol compounds. The two tetraketones were polymerized with three aromatic tetraamines, including 3,3′-diaminobenzidine (a), 3,3′,4,4′-tetraaminodiphenylether (b) and 3,3′,4,4′-tetraaminodiphenylsulfone (c), respectively to afford six thioether-bridged polyphenylquinoxalines (PPQs) – PPQ-1a–1c and PPQ-2a–2c. The obtained PPQs exhibited good solubility not only in conventional *m*-cresol and chloroform, but in the aprotic solvent – *N*-methyl-2-pyrrolidinone (NMP). PPQ-1c and 2c containing sulfone units were even soluble in tetrahydrofuran at room temperature with a solid content of 15 wt%. Flexible and tough PPQ films cast from their NMP solution showed good thermal stabilities, including glass transition temperatures in the range of 215–248 °C and 5% weight loss temperatures exceeding 500 °C in nitrogen. The PPQ films at a thickness of ~10 μm exhibited moderate optical transparency at 450 nm. The best optical transmittance around 80% was achieved by PPQ-1c and 2c containing electron-withdrawing sulfone moieties. The synergic effects of flexible thioether linkages and highly conjugated quinoxaline rings in the present PPQs endowed them with ultra-high refractive indices up to 1.7953 at 632.8 nm and birefringences close to zero.

1. Introduction

High refractive index (high-*n*) polymers have currently attracted much attention in fabricating high performance optoelectronic devices [1,2]. Polymer coatings with refractive index (*n*) higher than 1.70 are promising materials for a wide range of optoelectronic applications due to their great potential in improving the performance of the devices [3–6]. However, the *n* values of conventional polymers are usually lower than 1.70 [7]. Based on Lorentz–Lorenz equation [1], various methodologies have been now established to increase the *n* values of polymers beyond 1.70, including introduction of sulfur elements, halogens except fluorine, phosphorous components, metallic elements as well as other substituents with high molar refractions (R_M) and low molar volumes (V_M). Among the substituents, sulfur-containing groups, such as linear thioether (–S–), cyclic thioether (thiophene, thianthrene or thiadiazole) and sulfone (–SO_2–), seem to be the most optimal choices due to their combined advantages to develop high-*n* optical polymers. Thus, various sulfur-containing polymers, including poly(arylene sulfide), poly(ether sulfone), and poly(thioether ketone) [8–10] have been well investigated as high-*n* optical materials. In addition, aromatic, particularly heteroaromatic components are also beneficial to increase the polymers' *n* values. For instance, Ueda lab developed a series of sulfur-containing polyimides possessing *n* values as high as 1.77 at 632.8 nm [11–16].

Polyphenylquinoxaline (PPQ) is an important class of heteroaromatic polymer, first developed by Hergenrother in 1967 [17]. PPQ is characterized by its low moisture absorption, high thermal and hydrolytic stability; thus initially developed to serve as high-temperature repellent adhesives or composites to meet the severe demands of extreme environments [18–20]. Lately, various specific properties of PPQs have been gradually revealed, greatly expanding their applications in high-tech fields. Up to now, PPQs with various structural characteristics and functionalities have been developed. Systemic work includes the low-cost PPQs synthesized from self-polymerizable quinoxaline monomers developed by Harris group [21–25]; sulfonated PPQs for proton exchange membrane fuel cells [26,27]; and nanoporous PPQ foams as potential low-*k* interlayer dielectric materials for integrated circuit [28,29]. Recently, the applications of PPQs in optical fields have been increasingly investigated. Various electron-transporting PPQs [30–32] and nonlinear optical PPQs [33,34] were reported.

---

* Corresponding authors. Tel.: +86 10 62564819; fax: +86 10 62569562.
E-mail addresses: liujg@iccas.ac.cn (J.-g. Liu), shiyang@iccas.ac.cn (S.-y. Yang).

0032-3861/$ – see front matter © 2010 Elsevier Ltd. All rights reserved.
doi:10.1016/j.polymer.2010.06.035

Although PPQs have been widely evaluated as optical materials, to our knowledge, researches concerning refractive indices of the polymers have rarely been addressed until now. Actually, from the viewpoint of structure characteristics, there exists a high content of aromatic components with high molar refractions in PPQs, which might be propitious to increasing their *n* values. This fact attracted us to investigate the structure–refractive index relationships in PPQs. Our preliminary research has confirmed that ether-containing PPQs exhibited intrinsic high refractive indices and low birefringence [35]. Thus, as a part of our continuous endeavor to develop high-*n* polymers, the objective of the present work is to further increase the *n* values of PPQs by introduction of sulfur units. Meanwhile, the optical transparency of the PPQs in ultraviolet–visible light region was also taken into consideration. The synergic effects of thioether and quinoxaline ring on the solubility, thermal stability, especially refractive index and birefringence of the PPQs were investigated in detail.

2. Experimental

2.1. Materials

4-Nitrobenzil was synthesized in our laboratory according to the literature [36]. 4,4′-Thiobisbenzenethiol, 4,4′-thiodiphenol and 3,3′-diaminobenzidine (a) were purchased from Aldrich Chemical Co. and used as received. 3,3′,4,4′- Tetraaminodiphenylether (b) was synthesized according to the reported procedure [37]. 3,3′,4,4′-Tetraaminodiphenylsulfone (c) was kindly supplied by Konishi Chemical Ind. Co., Japan and recrystallized from acetonitrile before use. *N*-methyl-2-pyrrolidinone (NMP), dimethylsulfoxide (DMSO), *m*-cresol, *N*,*N*-dimethylacetamide (DMAc), cyclopentanone (CPA), tetrahydrofuran (THF) and other solvents were purified by distillation prior to use. The other commercially available reagents were used without further purification.

2.2. Measurements

Inherent viscosity was measured using an Ubbelohde viscometer with a 0.5 g/dL NMP solution at 25 °C. Absolute viscosity was measured using a Brookfield DV-II+ Pro viscometer at 25 °C. Gel permeation chromatography (GPC) measurements were performed using a Waters 1515 HPLC pump equipped with a Waters 2414 refractive index detector. Two Waters Styragel columns (HR 5E) kept at 35 °C ± 0.1 °C were used with HPLC grade tetrahydrofuran (THF) as the mobile phase at a flow rate of 1.0 mL/min. Fourier transform infrared (FT IR) spectra were obtained with a Tensor 27 Fourier transform spectrometer. Ultraviolet–visible (UV–vis) spectra were recorded on a Hitachi U-3210 spectrophotometer at room temperature. The cutoff wavelength was defined as the point where the transmittance drops below 1% in the spectrum. Prior to test, PPQ samples were dried at 100 °C for 1 h to remove the absorbed moisture. Nuclear magnetic resonances (^{1}H NMR and ^{13}C NMR) were performed on a AV 400 spectrometer operating at 400 MHz in DMSO-d_6 or $CDCl_3$. Differential scanning calorimetry (DSC) and thermogravimetric analysis (TGA) were recorded on a TA-Q series thermal analysis system at a heating rate of 10 °C/min and 20 °C/min in nitrogen or air, respectively. The tensile properties were performed on an Instron 3365 Tensile Apparatus with 80 × 10 × 0.05 mm^3 specimens in accordance with GB 1447-83 at a drawing rate of 2.0 mm/min. Seven samples of each PPQ film were tested. Dielectric constants (ε) were measured on a QBG-3B high-frequency Q meter in accordance with GB 1409-88 at 1 MHz at room temperature. Samples were dried at 120 °C for 1 h to eliminate absorbed moisture prior to testing.

Solubility was determined as follows: 1.5 g of the PPQ resin was mixed with 8.5 g of the tested solvent at room temperature (15 wt% solid content), which was then mechanically stirred in nitrogen for 24 h. The solubility was determined visually as three grades: completely soluble (++), partially soluble (+), and insoluble (−). The complete solubility is defined as a homogenous and clean solution is obtained, in which no phase separation, precipitation or gel formation is detected.

Refractive index of the PPQ film formed on a 3-inch silicon wafer was measured at room temperature with a prism coupler (Metricon, model PC-2010) equipped with a He–Ne laser light source (wavelength: 632.8 nm). The in-plane (n_{TE}) and out-of-plane (n_{TM}) refractive index were determined using linearly polarized laser light parallel (transverse electric, TE) and perpendicular (transverse magnetic, TM) polarizations to the film plane, respectively. In-plane (n_{TE})/out-of-plane (n_{TM}) birefringence (Δn) was calculated as a difference between n_{TE} and n_{TM}. The average refractive index (n_{av}) was calculated according to equation (1):

$$n_{av} = (2n_{TE} + n_{TM})/3 \tag{1}$$

2.3. Monomer synthesis

2.3.1. 4,4′-Thiobis[(p-phenyleneoxy)benzil] (STK, 1)

In a 500-mL three-necked flask equipped with a mechanical stirrer, a nitrogen inlet, and a condenser, a mixture of 4-nitrobenzil (53.60 g, 0.21 mol), 4,4′-thiodiphenol (21.8 g, 0.1 mol), and anhydrous DMSO (240 mL) was heated to 60 °C. Then, anhydrous potassium carbonate (69.11 g, 0.5 mol) was added. The reaction was maintained at 60 °C for 20 h. Upon confirmation of the completion of the reaction by thin-layer chromatography, the solution was cooled to room temperature and then poured into a mixed solvent containing hydrochloric acid (1 mol/L, 2400 mL) and chloroform (600 mL). The organic phase was collected and washed thoroughly with deionized water. Then, the chloroform solution was dried with $MgSO_4$. After distilling off the solvent, a pale-yellow solid was obtained. The crude product was purified by a two-step recrystallizations, first from acetic acid and then from a mixture of benzene–ethanol (4:3, v/v). The purified tetraketone STK was obtained as pale-yellow crystals (39.55 g, yield: 62.3%).

Melting point: 127.5 °C (DSC peak temperature). FT IR (KBr, cm^{-1}): 1672, 1600, 1582, 1483, 1248, 1163 and 881. ^{1}H NMR ($CDCl_3$): 7.04–7.08 (m, 8H), 7.39–7.42 (d, 4H), 7.51–7.55 (t, 4H), 7.66–7.70 (t, 2H), and 7.97–7.99 (m, 8H). ^{13}C NMR ($CDCl_3$): 117.3, 120.6, 127.4, 128.5, 129.4, 131.4, 131.9, 132.5, 132.6, 134.4, 153.9, 162.5, 192.4, and 193.9. Mass [m/e (relative intensity)]: 529 (M$^+$-105, 100). Elemental analysis: calculated for $C_{40}H_{26}O_6S$: C, 75.70%; H, 4.13%. Found: C, 75.46%; H, 4.09%.

2.3.2. 4,4′-Thiobis[(p-phenylenesulfanyl)benzil] (3STK, 2)

The monomer was similarly synthesized by the procedure as STK except that 4,4′-thiobisbenzenethiol was used instead of 4,4′-thiodiphenol.

Melting point: 158.9 °C (DSC peak temperature). FT IR (KBr, cm^{-1}): 1666, 1585, 1473, 1215, 1176 and 878. ^{1}H NMR (DMSO-d_6): 7.35–7.37 (d, 4H), 7.45–7.47 (d, 4H), 7.55–7.57 (d, 4H), 7.60–7.64 (t, 4H), 7.77–7.81 (t, 2H), 7.84–7.86 (d, 4H), and 7.89–7.91 (d, 4H). ^{13}C NMR ($CDCl_3$): 127.6, 129.0, 129.9, 130.4, 130.7, 132.0, 132.9, 134.7, 134.9, 136.6, 147.1, 193.3, and 194.3. Mass [m/e (relative intensity)]: 561 (M$^+$105, 100). Elemental analysis: calculated for $C_{40}H_{26}O_4S_3$: C, 72.05%; H, 3.93%. Found: C, 71.76%; H, 3.88%.

2.4. Polymer synthesis and film preparation

Six PPQs, including PPQ-1a–1c based on STK and PPQ-2a–2c based on 3STK were synthesized via a two-step procedure with *m*-cresol as the solvent (Scheme 2). As a typical embodiment, PPQ-2c was synthesized according to the procedure as follows. To a stirred solution of 3,3′-diaminobenzidine (a) (4.2854 g, 0.02 mol) in *m*-cresol (50 g), 3STK (13.3364 g, 0.02 mol) was gradually added. An additional volume of *m*-cresol (20 g) was added to wash the residual monomers, and at the same time to adjust the solid content of the reaction system to be 20 wt%. The mixture was stirred at room temperature for 24 h under a nitrogen flow to form a viscous brown solution. Then, the reaction mixture was heated to 120 °C and maintained for another 4 h. The obtained viscous pale-brown solution was cooled to room temperature and slowly precipitated in an excess of methanol (500 mL). The yellow, fibrous PPQ-2c resin was collected by filtration. The resin was further heated in methanol with refluxing for 24 h, then, dried at 80 °C in vacuum overnight. Yield: 15.21 g (94%).

A PPQ-2c resin (1.5 g) was dissolved in NMP (8.5 g) at room temperature to afford a 15 wt% solution. The solution was filtered through a 0.45 μm Teflon syringe filter to remove any undissolved impurities. Then, the solution was spin-coated on a clean silicon wafer or quartz substrate. The thickness of the PPQ film was controlled by regulating the spinning rate. PPQ-2c films with thicknesses from 10 to 100 μm were obtained by thermally baking the solution in flowing nitrogen according to the following heating procedure: 80 °C/2 h, 150 °C/1 h, 200 °C/1 h, and 250 °C/1 h.

The other PPQ resin and films were prepared according to a similar procedure as mentioned above.

3. Results and discussion

3.1. Monomer synthesis

The synthesis route of the novel tetraketones incorporating thioether linkages in the main chain is shown in Scheme 1. The target compounds were easily synthesized by the nitro nucleophilic substituent reaction of 4-nitrobenzil with 4,4′-thiodiphenol for STK and 4,4′-thiobisbenzenethiol for 3STK with good yields. The nitro group in 4-nitrobenzil was activated by the *para*-substituted electron-withdrawing C_6H_5COCO-group [38], thus its nucleophilic substituent reaction proceeded smoothly under a moderate condition. Fig. 1 shows the FT IR spectra of the tetraketones, in which the characteristic bands of carbonyl groups in benzil moiety were both clearly observed at 1672 cm^{-1} for STK and 3STK.

The ^1H and ^{13}C NMR spectra of the monomers are shown in Figs. 2 and 3, respectively, together with the assignments of the observed resonances. As shown in Fig. 2, the protons *ortho* to the electron-withdrawing carbonyl (H_c and H_d) appeared at the lowest field in both of the spectra. In Fig. 2a, the protons *ortho* to the ether bond (H_e and H_f) resonated at the highest field in the spectrum. However, when the ether bond was replaced by thioether bond, the resonances apparently changed. It can be clearly seen in Fig. 2b that the chemical shifts of H_e and H_f were higher than that of H_g in 3STK, which was contrary to that in STK (Fig. 2a). This is mainly attributed to the relatively high electron-withdrawing characteristics of thioether compared to oxygen–ether unit [39]. This variety was also clearly reflected in the ^{13}C NMR spectra of the monomers. As depicted in Fig. 3, for both compounds, 14 signals are clearly revealed due to the structure symmetry; among these, 7 carbons induce signals in the DEPT-135 measurements due to the existence of the attached protons. This result is consistent with the proposed structures. The variety of chemical shift sequences of C_{11} and C_{12} in Fig. 3a and b reflects the effects of oxygen–ether and thioether units on the structures of the monomers.

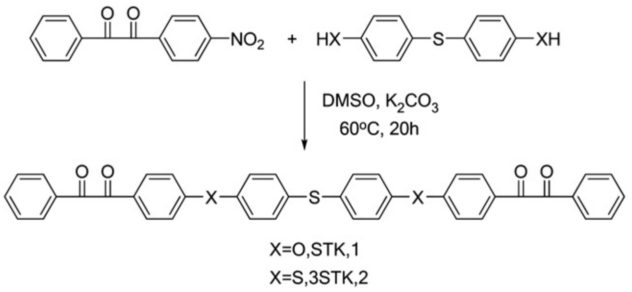

Scheme 1. Synthesis of sulfur-containing tetraketones.

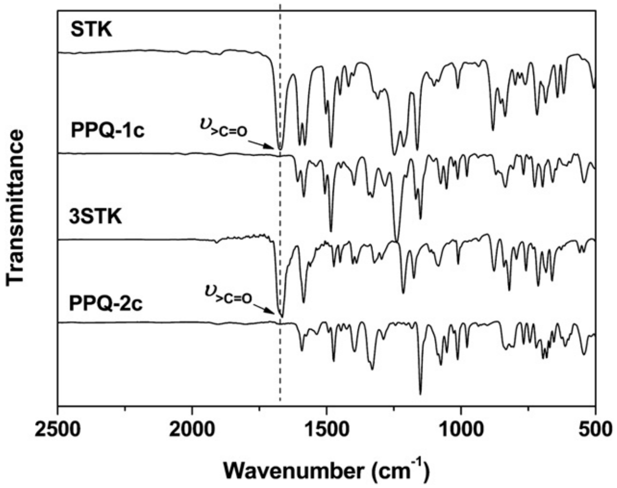

Fig. 1. FT IR spectra of tetraketones and PPQs.

In addition, elemental analysis results also supported the successful preparation of the target tetraketone compounds.

3.2. Polymer synthesis

Six PPQs were prepared via a two-step polycondensation procedure shown in Scheme 2. It has been well established that the solution polymerization reaction of tetraketones and tetraamines was strongly dependent on the monomer reactivity and the

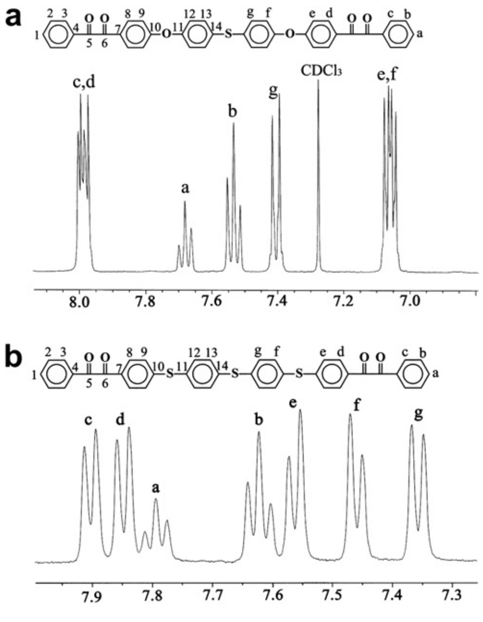

Fig. 2. ^1H NMR spectra of tetraketones. (a) STK ($CDCl_3$); (b) 3STK (DMSO-d_6).

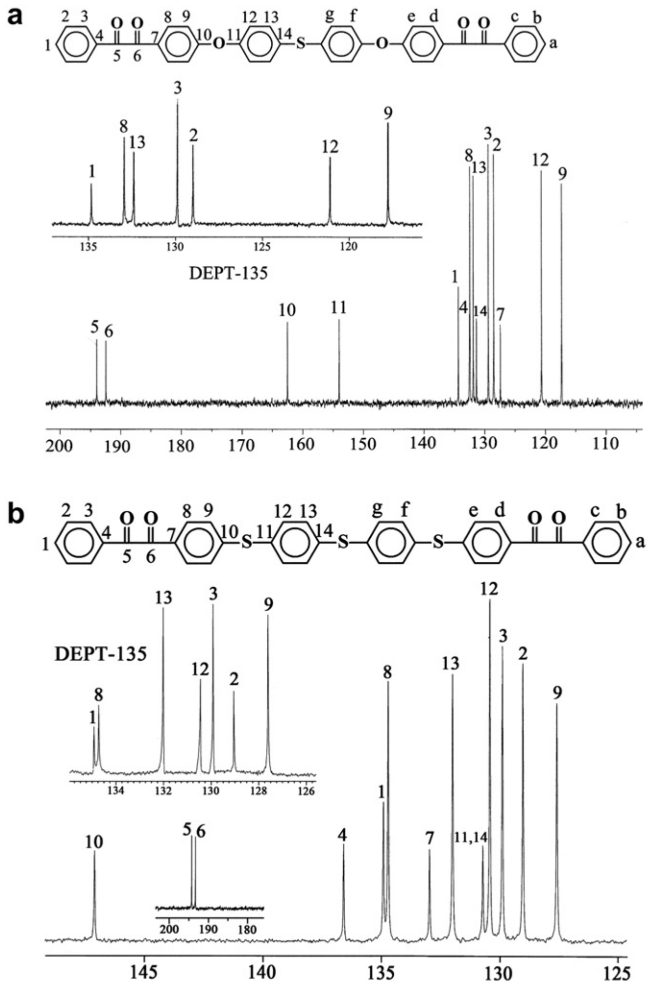

Fig. 3. ^{13}C NMR spectra of tetraketones (DMSO-d_6). (a) STK; (b) 3STK (DEPT-135 was embedded).

solubility of the obtained PPQs in the reaction medium. For instance, Wrasidlo synthesized a series of high molecular weight soluble PPQs containing flexible groups at ambient temperature [40]. However, in some other reports, higher polymerization temperature (>100 °C) had to be adopted [41]. In the present work, the reactivity of amino groups in 3,3′,4,4′-tetraaminodiphenylsulfone was decreased by the electron-withdrawing sulfone groups. Thus, a two-step polymerization procedure, including an initial reaction at room temperature for 24 h, and a following reaction at 120 °C for another 4 h was utilized.

As tabulated in Table 1, PPQs with inherent viscosities ranging from 0.73 to 0.85 dL/g were obtained, indicating the feasibility of the polymerization conditions and high purity of the monomers. The average molecular weights of PPQ-1c and 2c were determined by GPC with THF as an eluent and polystyrene standards as the reference. The GPC plots of PPQ-1c and PPQ-2c are shown in Fig. 4, in which the number average molecular weights (M_n), weight average molecular weights (M_w) and the polydispersity indices (PDIs) of the polymers are inserted. According to the data, the PPQs exhibited moderate M_n values around 11,000 and M_w around 15,000. This corresponds to the average degree of polymerization of 13 and PDI around 1.3. The somewhat low molecular weight values might be ascribed to the low reactivity of amino groups in 3,3′,4,4′-tetraaminodiphenylsulfone. Self-standing PPQ films, including thin films (thickness: ~10 μm) for IR and UV measurements and thick ones (thickness: 30–50 μm) for thermal and mechanical evaluations were prepared by spin-coating the PPQ-NMP solutions on silicon wafer. After curing, flexible and tough PPQ films were obtained.

The structures of the PPQ films were confirmed by FT IR measurements. Fig. 1 shows the typical FT IR spectra of the polymers. The characteristic absorptions of carbonyl in STK and 3STK located at 1672 cm^{-1} disappear in the spectra of PPQ-1c and PPQ-2c, indicating the complete conversion from the monomers to polymers. Meanwhile, the characteristic bands due to sulfone (SO_2) groups at 1320 and 1160 cm^{-1} are observed in both of the polymers. In addition, the typical absorptions of thioether (Ar–S–Ar) linkages appear at 1257 cm^{-1} in the spectra.

In Section 3.1, we discussed the effects of oxygen–ether and thioether groups on the absorptions of protons in STK and 3STK. Similar effects were also observed in PPQs, as illustrated in Fig. 5. Both of the ^{1}H NMR spectra of PPQ-1c and PPQ-2c are clearly divided into two parts. The lower fields were occupied by the absorptions of protons in the tetraamine moiety (H_a, H_b, and H_c) due to the electron-withdrawing quinoxaline ring and sulfone unit. In the higher fields, the effects of structure variety on the absorptions of the protons (H_e, H_f, and H_g) were obviously revealed.

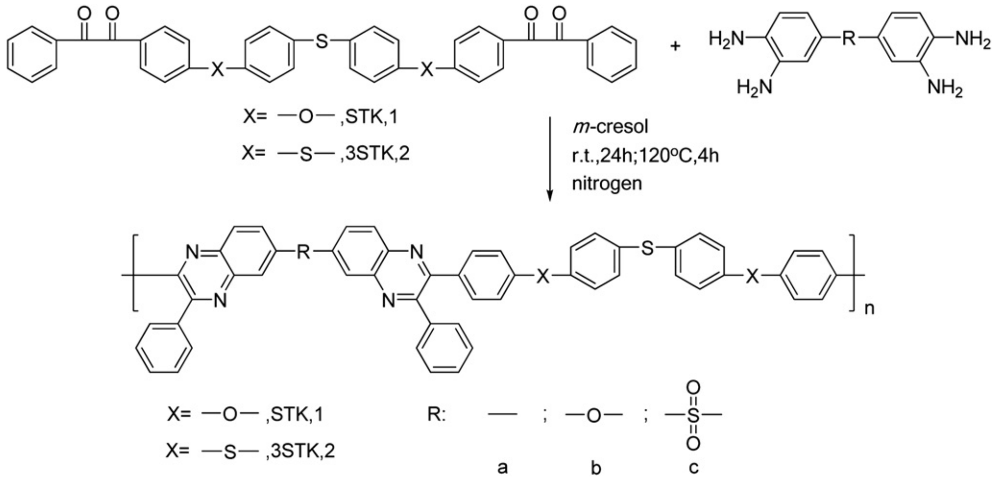

Scheme 2. Synthesis of PPQ-1a–1c and PPQ-2a–2c.

Table 1
Inherent viscosities and solubility of PPQs.

Sample	$[\eta]_{inh}$[a] (dL/g)	Solvent[b]						
		NMP	DMAc	*m*-cresol	CPA	THF	$CHCl_3$	Ethanol
PPQ-1a	0.85	++	+	++	−	−	++	−
PPQ-1b	0.82	++	+	++	−	+	++	−
PPQ-1c	0.77	++	++	++	+	++	++	−
PPQ-2a	0.83	++	+	++	−	−	++	−
PPQ-2b	0.79	++	+	++	−	+	++	−
PPQ-2c	0.73	++	++	++	+	++	++	−

[a] Inherent viscosities measured with a PPQ resin at a concentration of 0.5 g/dL in NMP at 25 °C.

[b] ++: Wholly soluble at room temperature; +: partially soluble; −: insoluble; CPA: cyclopentanone.

3.3. Solubility

The solubility of PPQs is summarized in Table 1. As we know, the commercial available PPQ – IP 200® PPQ was only soluble in phenol and its derivatives. Although it is also soluble in chloroform and 1,1,2,2-tetrachloroethane, insoluble gels often form during storage [20]. The potential hazards of phenol solvents to environments and operators limited the wide applications of IP 200® PPQ. Enhancement of solubility of PPQs in common low-toxic solvents, such as NMP has been successfully achieved by introduction of flexible ether substituents or bulky alkyl groups in our previous work [35].

Similarly, in the present work, all the PPQs were easily soluble in NMP, *m*-cresol, and chloroform at a concentration of 15 wt%. Among the PPQs, 1c and 2c showed the best solubility due to the presence of bulky sulfone units. They were also wholly soluble in DMAc and THF and partially soluble in CPA.

The better solubility of 1c and 2c could be further ascertained by the absolute viscosities (η) of the polymers. Fig. 6 illustrates the correlations between the η values and solid contents of PPQ-2a–2c. NMP was used as the solvent. Although all the PPQs were soluble in NMP, the η values were quite different. For instance, at the same solid content of 20 wt%, PPQ-2c had a η value of 18,917 mPa s, which was much lower than that of PPQ-2a (51,023 mPa s). The relatively lower η values of PPQ-2c indicate its higher solvability in the solvent. The good solubility is mainly attributed to the synergic effects of flexible thioether linkages, lateral phenyl groups, bulky sulfone moieties and quinoxaline rings. The good solubility of the present PPQs in low-toxic solvents facilitates their applications in high-tech fields.

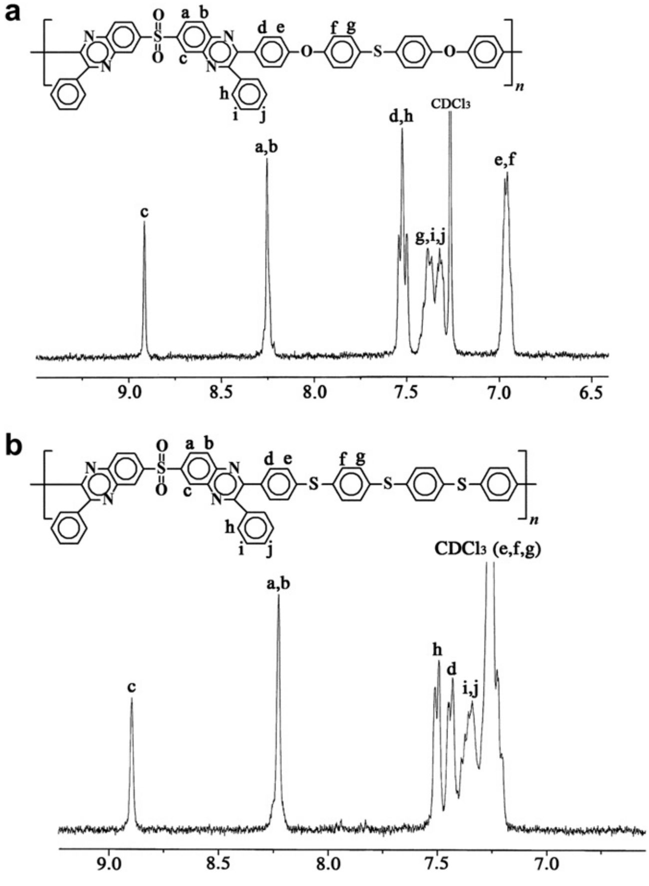

Fig. 5. ^{1}H NMR spectra of PPQs ($CDCl_3$). (a) PPQ-1c; (b) PPQ-2c.

3.4. Thermal and mechanical properties

The thermal properties of PPQs were investigated by thermogravimetric analysis (TGA) and differential scanning calorimetry (DSC) measurements and the results are presented in Table 2. TGA curves (Fig. 7) reveal several structure–thermal stability correlations of the PPQ films. First, all the polymers exhibit good thermal stability up to 500 °C both in nitrogen and in air, which is mainly ascribed to the highly-conjugated quinoxaline rings. Secondly,

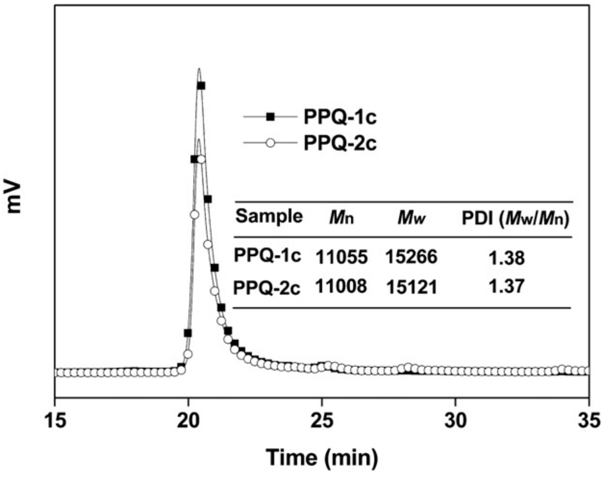

Sample	*M*n	*M*w	PDI (*M*w/*M*n)
PPQ-1c	11055	15266	1.38
PPQ-2c	11008	15121	1.37

Fig. 4. GPC plots and molecular weights of PPQ-1c and PPQ-2c.

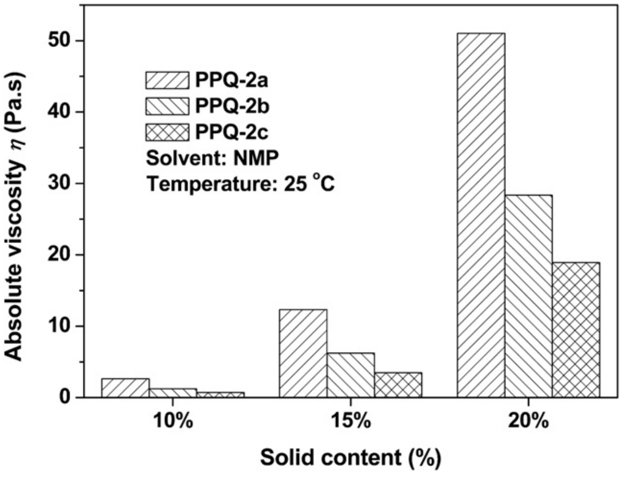

Fig. 6. Correlations of absolute viscosities (η) and solid contents of PPQ-2a–2c.

Table 2
Thermal and mechanical properties of PPQ films.

Sample	T_g[a] (°C)	$T_{5\%}$[a] (°C)	$T_{10\%}$[a] (°C)	R_{w750}[a] (%)	T_s[c] (MPa)	E_b[c] (%)	T_M[c] (GPa)
PPQ-1a	248	559 (560)[b]	570 (584)	68 (2.2)	81	6.0	2.1
PPQ-1b	221	551 (537)	562 (573)	62 (0.7)	76	6.3	2.1
PPQ-1c	244	502 (527)	526 (552)	56 (3.7)	72	5.4	2.2
PPQ-2a	235	537 (547)	552 (586)	67 (2.7)	86	6.2	2.3
PPQ-2b	215	545 (546)	554 (560)	61 (1.1)	73	5.8	2.1
PPQ-2c	230	500 (520)	523 (548)	57 (3.7)	71	5.2	2.3

[a] T_g: glass transition temperature; $T_{5\%}$, $T_{10\%}$: temperatures at 5% and 10% weight loss, respectively; R_{w750}: residual weight ratio at 750 °C.
[b] The thermal data measured in air.
[c] T_s: tensile strength; E_b: elongation at break; T_M: tensile modulus.

PPQs derived from sulfone-bridged tetraamine (PPQ-1c and 2c) exhibit lower thermal stability compared to their ether-linked (PPQ-1b and 2b) and biphenyl (PPQ-1a and 2a) analogs. The unstable nature of sulfone groups at elevated temperatures has been observed in other polymers [15]. Thirdly, most of the PPQs show higher initial thermal decomposition temperatures in air than those in nitrogen. For instance, the 5% weight loss of PPQ-2c occurred at 500 °C in nitrogen, which was 20 °C lower than that in air (520 °C). This phenomenon has also been reported on the other sulfur-containing polymers in the literature [39,42]. In Ref. [42], the authors investigated the thermal decomposition of poly(phenylene sulfide) (PPS) film under different atmospheres using a high-resolution thermogravimetry analyzer. They observed that the thermal decomposition temperatures of PPS increased in the following order: in helium < in nitrogen < in argon < in air. The char yield at 700 °C increased in the order: in air < in helium < in nitrogen < in argon. The author ascribed this phenomenon to the different thermal conductivities and densities of the gases. In the present investigation, with the increase of the temperatures, the PPQ samples exhibited more rapid decomposition behavior in air, leaving little residues at 750 °C. This phenomenon is consistent with the literature.

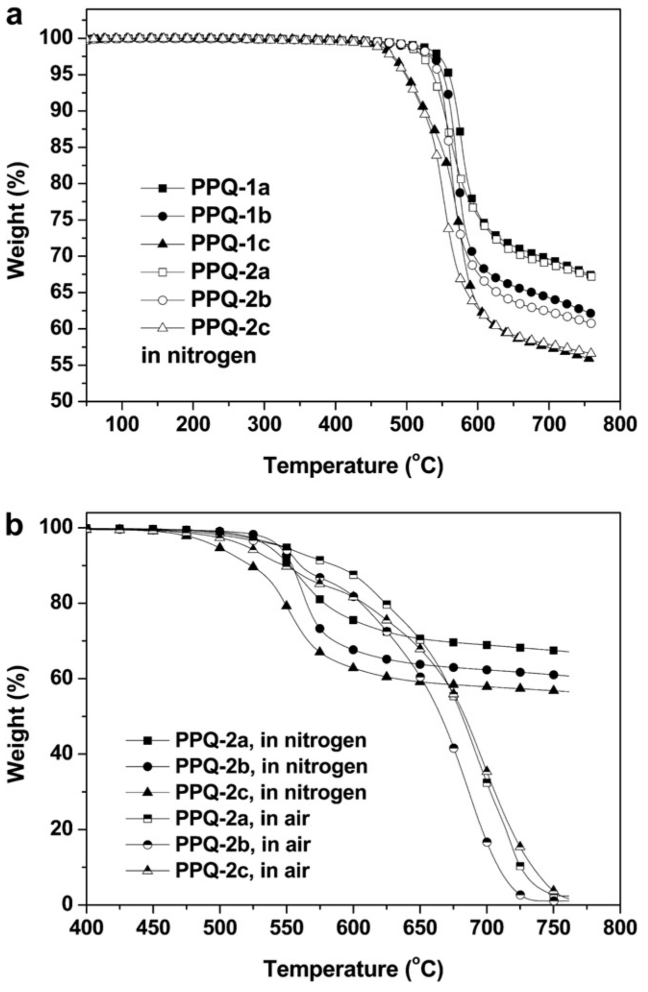

Fig. 7. TGA curves of PPQ films (a) in nitrogen; (b) PPQ-2a–2c in nitrogen and air (heating rate: 20 °C/min).

The glass transition temperature (T_g) values of the PPQs are in the range of 215–248 °C, as shown in Fig. 8 and Table 2. These values are much lower than that of the standard PPQ (IP 200® PPQ; $T_g = 317$ °C) [20] due to the existence of flexible thioether linkages. For the same tetraketone, the T_g values of the PPQs decreased in the following order: PPQ-a > PPQ-c > PPQ-b. This trend, on one hand, depends on the rigidity of the linkages in the tetraamine moiety; on the other hand, the molecular volumes of the bridges. The bulky sulfone (SO_2) segments are less prone to move at elevated temperatures in comparison with ether segments, resulting in higher T_g values.

The tensile properties of the PPQ films are listed in Table 2. The isotropic films exhibited acceptable properties with the tensile strength higher than 70 MPa, tensile modulus higher than 2.1 GPa, and the elongation in the range of 5.2–6.3%.

3.5. Optical properties

As mentioned in Introduction, standard PPQs were initially designed as high-temperature resistant adhesives or composites for applications in extreme environments. Thus, highly conjugated and fused structures were preferred. These structures afford conventional PPQs good thermal and environmental stability, however, greatly sacrifice their optical transparency in the visible light region. It has been well-known that introduction of flexible spacers, such as ether (—O—), thioether (—S—), and methylene (—CH_2—) in heteroaromatic polymers would be beneficial to separating the chromophoric groups and disturbing the intramolecular conjugation interactions, thus, be helpful for the penetration of visible light. In addition, some external factors including the purity of the PPQ resin, residual solvent in the resin, and film-forming history might also affect the colors of the PPQ films.

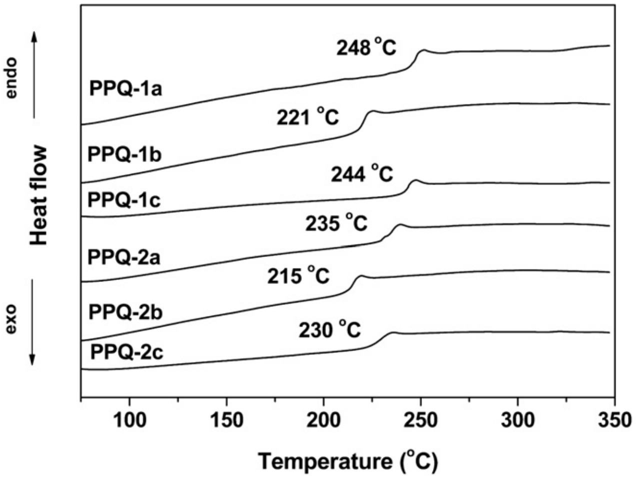

Fig. 8. DSC curves of PPQ films (heating rate: 10 °C/min, nitrogen).

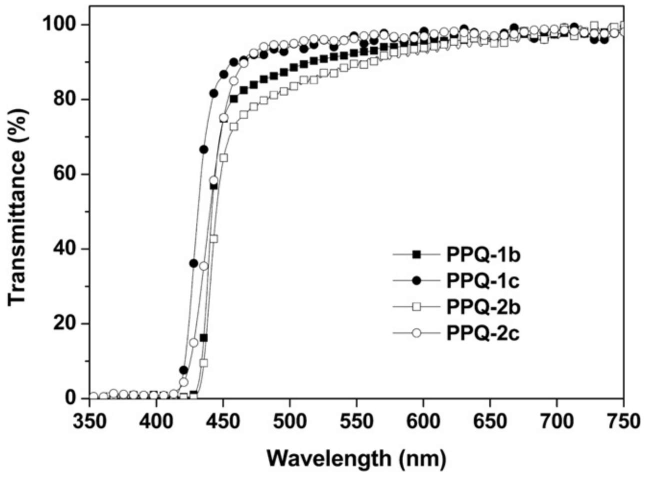

Fig. 9. UV–Vis spectra of PPQ films (thickness: ~10 μm).

Fig. 9 shows the typical UV–Vis spectra of PPQ films. The cutoff wavelengths (λ) and transmittances at 450 nm (T_{450}) are summarized in Table 3. The PPQ films (thickness: ~10 μm) were cast in an oven filled with flowing nitrogen at curing temperatures up to 250 °C. No apparent weight loss was detected before 300 °C in TGA measurements, indicating a low content of residual NMP. The obtained films exhibited colors ranging from pale-yellow (1c and 2c) to pale-brown (1a and 2a) depending on their structures. In each series, PPQ-1c and 2c showed the best optical transmittances due to the existence of electron-withdrawing sulfone moiety. For instance, the T_{450} value of PPQ-1c is 86%, which is 12% and 24% higher than that of PPQ-1b and PPQ-1a, respectively. In addition, the λ values of PPQ-1c (406 nm) and 2c (412 nm) are the shortest in the series, indicating their superior optical transparency in a wider spectra range.

The PPQ samples for refractive index measurements were prepared by spin-coating on a quartz substrate. The thickness of the films ranged from 4.6 to 7.9 μm. The refractive indices measured at 632.8 nm wavelength are summarized in Table 3. The n_{av} values ranging from 1.7277 (PPQ-1b) to 1.7953 (PPQ-2a) make the present PPQs rank first in the families of high-*n* polymers in the literature. In our previous work [35], a maximum *n* value of 1.7739 was achieved by a PPQ derived from 4,4′-bis(4-benzilyloxy)biphenyl and 3,3′-diaminobenzidine (PPQ-II$_a$). In the present work, the value was increased by 0.0214 (1.7953 for PPQ-2a). Considering the same tetraamine moiety in PPQ-II$_a$ and PPQ-2a, the improvement of *n* could mainly be attributed to the contribution of sulfur components in the tetraketone moiety.

The n_{av} values of the PPQs decrease in the order of 2a > 1a > 2c > 2b > 1c > 1b. This sequence well reflects the general trends for the specific structural compositions of the PPQs. First, the PPQs with higher sulfur contents generally exhibited higher n_{av} values. For instance, the n_{av} values of 3STK-PPQs (1.7590–1.7953) are correspondingly higher than those of their STK-based analogs (1.7277–1.7665).

Secondly, in each series, the highest n_{av} value was achieved by the polymer derived from 3,3′-diaminobenzidine (a) despite its relatively lower sulfur content in comparison with the polymer from 3,3′,4,4′-tetraaminodiphenylsulfone (c). For instance, PPQ-2a has a n_{av} value of 1.7953, which is 0.0347 higher than that of PPQ-2c, although the former's sulfur content (11.89%) is lower than that of the latter (14.69%). This fact indicates that the solid state structures of PPQs including chain rigidity and degrees of molecular packing should play an important role in affecting the refractive index of the polymers [43]. Actually, it has been well established that the refractive index of one polymer is the result of competition among several factors, including molecular polarizability, chain flexibility, molecular geometry and orientation in the polymer backbone [44]. For thioether substituents, the dominant factor affecting the *n* values is their high molar refractions. However, for sulfone group, its contribution to *n* values of the polymers includes not only its high molar refraction but its high molar volume. These two interinhibitive factors usually bring a more complex influence on the *n* values of the polymers. For instance, for PPQ-2c, the looser molecular packing originating from the bulky sulfone groups in the tetraamine moiety decreases its refractive index despite the existences of high molar refraction thioether groups in the tetraketone moiety. On the contrary, for PPQ-2a, the higher molecular packing density of the molecular chains induced by the rigid biphenyl unit in the tetraamine moiety and the high molar refractions caused by the thioether linkages in the tetraketone moiety synergistically endow the polymer with the highest n_{av} value among the PPQs. Actually, from another point of view, PPQ-2c has the best optical transparency among the 3STK-PPQs, revealing the lowest degree of molecular packing in the polymer.

Thirdly, the PPQ films exhibited good optical isotropic characteristics as evidenced by the small birefringence values. The facts that the n_{TE} values are slightly higher than n_{TM} ones reflect the slight chain orientation parallel to the film plane. Such small birefringences can mainly be contributed to the small polarizability anisotropy of quinoxaline rings and the low degree of molecular orientation due to the flexible thioether linkages in the molecular chains [45].

Table 3
Optical properties of the PPQ films.

Sample	S_C[a] (%)	λ[b] (nm)	T_{450}[c] (%)	d[d] (μm)	Refractive indices at 632.8 nm				ε[f]
					n_{TE}[e]	n_{TM}[e]	n_{av}[e]	Δ*n*[e]	
PPQ-1a	4.13	426	62	6.4	1.7667	1.7662	1.7665	0.0005	3.12 (3.24)[g]
PPQ-1b	4.04	424	74	4.6	1.7278	1.7276	1.7277	0.0002	2.98 (3.15)
PPQ-1c	7.62	406	86	6.6	1.7296	1.7293	1.7295	0.0003	2.99 (3.08)
PPQ-2a	11.89	429	56	7.9	1.7954	1.7950	1.7953	0.0004	3.22 (3.28)
PPQ-2b	11.66	428	64	7.3	1.7590	1.7589	1.7590	0.0001	3.09 (3.19)
PPQ-2c	14.69	412	78	6.2	1.7607	1.7605	1.7606	0.0002	3.10 (3.17)

[a] Sulfur content.
[b] Cutoff wavelength.
[c] Transmittance at 450 nm.
[d] Film thickness for refractive index measurements.
[e] See Section 2.2.
[f] Estimated dielectric constant from Maxwell's equation as $\varepsilon = n_{av}^2$.
[g] Experimental dielectric constants.

The optical dielectric constants (ε) estimated roughly from the n_{av} values according to Maxwell's equation, $\varepsilon = n_{av}^2$ and the experimental values are both shown in Table 3. As expected, there two series of ε values revealed the similar trend. PPQ film with a higher n_{av} value usually exhibits a higher ε value. For example, PPQ-2a has a maximum ε value of 3.28, which is 0.20 higher than the minimum value of PPQ-1c.

The ε values of the PPQs are a bit lower than those of the wholly aromatic polyimides ($\varepsilon = 3.5–3.6$) [20]. Moreover, the present PPQs can be processed with their fully cyclized form in organic solvents. Thus, the good combined properties make the present PPQs good candidates not only for optoelectronic fabrication, but for advanced microelectronic assembly.

4. Conclusions

In order to develop polymers with extreme high refractive indices, a series of PPQs containing thioether moieties were synthesized. The introduction of thioether groups indeed increased the *n* values of the PPQ matrix. Refractive index up to 1.7953 is one of the highest values reported in the literature so far. Introduction of sulfone (SO_2) moiety in PPQs apparently improved their optical transparency, however, the refractive indices were somewhat sacrificed. The future work will focus on improving the sulfur contents of tetraketones via combination of high sulfur content groups, such as thianthrene. At the same time, the sulfone group will be preserved in the molecular structure of the PPQ. Thus, the new polymer might simultaneously exhibit extreme high refractive index, low birefringence and good optical transparency. Hopefully, the conclusion of the present work might provide a new insight in understanding the nature of the "age-old" polymer-PPQ and also a new path to develop polymers with extreme high-*n* values.

Acknowledgments

The authors greatly appreciate the financial supports from National Nature Science Foundation of China (NSFC) (No. 50873104).

References

[1] Liu JG, Ueda M. J Mater Chem 2009;19:8907–19.
[2] Lü CL, Yang B. J Mater Chem 2009;19:2884–901.
[3] Su HW, Chen WC. J Mater Chem 2008;18:1139–45.
[4] Chang CC, Chen WC. J Polym Sci Part A Polym Chem 2001;39:3419–27.
[5] Morford RV, Mercado RL, Planje CE, Flaim TD. Proc SPIE 2005;5724:34–41.
[6] Nakamura T, Fujii H, Juni N, Tsutsumi N. Opt Rev 2006;13:104–10.
[7] Brandrup J, Immergut EH, Gruike EA, Abe A, Bloch DR, editors. Polymer handbook. 4th ed. New York: John Wiley & Sons; 2005.
[8] Robb MJ, Knauss DM. J Polym Sci Part A Polym Chem 2009;47:2453–61.
[9] Okutsu R, Suzuki Y, Ando S, Ueda M. Macromolecules 2008;41:6165–8.
[10] Seesukphronrarak S, Kawasaki S, Kobori K, Takata T. J Polym Sci Part A Polym Chem 2007;45:3073–82.
[11] You NH, Nakamura Y, Suzuki Y, Higashihara T, Ando S, Ueda M. J Polym Sci Part A Polym Chem 2009;47:4886–94.
[12] Liu JG, Nakamura Y, Shibasaki Y, Ando S, Ueda M. J Polym Sci Part A Polym Chem 2007;45:5606–17.
[13] Terraza CA, Liu JG, Nakamura Y, Shibasaki Y, Ando S, Ueda M. J Polym Sci Part A Polym Chem 2008;46:1510–20.
[14] Liu JG, Nakamura Y, Shibasaki Y, Ando S, Ueda M. Macromolecules 2007;40:4614–20.
[15] Liu JG, Nakamura Y, Suzuki Y, Shibasaki Y, Ando S, Ueda M. Macromolecules 2007;40:7902–9.
[16] Liu JG, Nakamura Y, Ogura T, Shibasaki Y, Ando S, Ueda M. Chem Mater 2008;20:273–81.
[17] Hergenrother PM, Levine HH. J Polym Sci Part A-1 1967;5:1453–66.
[18] Hergenrother PM. Polym Eng Sci 1976;16:303–8.
[19] Lindley PM, Reinhardt BA. J Polym Sci Part A Polym Chem 1991;29:1061–71.
[20] Rabilloud G. High performance polymers. 2. Polyquinoxalines and polyimides: chemistry and applications. Paris: Editions Technip; 1999.
[21] Kim BS, Korleski JE, Zhang Y, Klein DJ, Harris FW. Polymer 1999;40:4553–62.
[22] Klein DJ, Modarelli DA, Harris FW. Macromolecules 2001;34:2427–37.
[23] Klein DJ, Korleski JE, Harris FW. J Polym Sci Part A Polym Chem 2001;39:2037–42.
[24] Baek JB, Harris FW. J Polym Sci Part A Polym Chem 2005;43:78–91.
[25] Baek JB, Harris FW. J Polym Sci Part A Polym Chem 2004;42:6318–30.
[26] Rusanov AL, Belomoina NM, Bulycheva EG, Yanul NA, Likhatchev DY, Dobrovolskii YA, et al. High Perform Polym 2008;20:627–41.
[27] Gong FX, Li NW, Zhang SB. Polymer 2009;50:6001–8.
[28] Merlet S, Marestin C, Romeyer O, Mercier R. Macromolecules 2008;41:4205–15.
[29] Merlet S, Marestin C, Schiets F, Romeyer O, Mercier R. Macromolecules 2007;40:2070–8.
[30] Kulkarni AP, Tonzola CJ, Babel A, Jenekhe SA. Chem Mater 2004;16:4556–73.
[31] Jandke M, Strohriegl P, Berleb S, Werner E, Brütting W. Macromolecules 1998;31:6434–43.
[32] Jung SH, Suh DH, Cho HN. Polym Bull 2003;50:251–8.
[33] Zhan XW, Liu YQ, Zhu DB, Xu G, Liu XC, Ye PX. Appl Phys A 2003;77:375–8.
[34] Gubbelmans E, Broeck KVD, Verbiest T, Beylen MV, Persoons A, Samyn C. Eur Polym J 2003;39:969–76.
[35] Li C, Li Z, Liu JG, Yang HX, Yang SY. J Macromol Sci Part A Pure Appl Chem 2010;47:248–53.
[36] Aldgate EC. J Chem Soc 1911;99:344–8.
[37] Foster R, Marvel CS. J Polym Sci Part A 1965;3:417–21.
[38] Relles HM, Orlando CM, Heath DR, Schluenz RW, Manello JS, Hoff S. J Polym Sci Polym Chem Edition 1977;15:2441–51.
[39] Liu JG, Shibasaki Y, Ando S, Ueda M. High Perform Polym 2008;20:221–37.
[40] Wrasidlo W, Augl JM. Macromolecules 1970;3:544–7.
[41] Keshtov ML, Mal'tsev EI, Lypenko DA, Brusentseva MA, Sosnovyi MA, Vasnev VA, et al. Polym Sci Ser B 2007;49:75–9.
[42] Li XG, Huang MR, Bai H, Yang YL. J Appl Polym Sci 2002;83:2053–9.
[43] Hanisch G, Podgorsek RP, Franke H. Sensors Actuators 1998;B51:348–54.
[44] Han KS, Jang WH, Rhee TH. J Appl Polym Sci 2000;77:2172–7.
[45] Badarau C, Wang ZY. Macromolecules 2004;37:147–53.